

New Perspectives in Molecular Imaging of Cardiovascular Diseases

F. Garibaldi - INFN - Roma1

- molecular imaging: the role of radionuclides techniques
- building an open, flexible system
- cardiovascular diseases (diagnosis and therapy)
 - detecting vulnerable atherosclerotic plaque
 - stem cell therapy of heart infarction
- conclusions and outlook

Collaboration

Istituto Superiore di Sanita'

E. Cisbani

S. Colilli

R. Fratoni

F. Garibaldi

TESA

M. Gricia

M. Lucentini

F. Santavenere

S. Torrioli

Farmaco

G. Marano

M. Musumeci

Farmaco

Ematologia

M. Baiocchi

Oncologia

L. Vitelli

INFN - Roma1

F. Cusanno

M.L. Magliozzi

Jefferson Lab (DOI)

S. Majewski

D. Weisemberger

B. Kross

J. Proffit

Johns Hopkins University

B.Tui

Y Wang

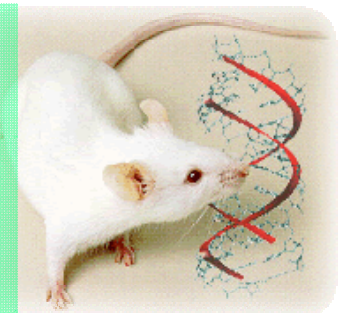
University of Rome

G. De Vincentis

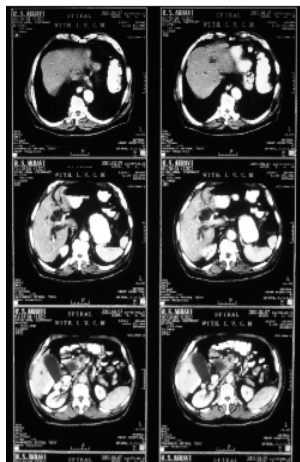
Molecular Imaging

- "... the *in vivo* characterization and measurement of biologic processes at the cellular and molecular level.
- - It sets forth to probe the molecular abnormalities that are the basis of disease rather than to image the end effects of these molecular alterations.
- Imaging of specific molecular targets enables:
 - ✓ earlier detection and characterization of disease;
 - ✓ earlier and direct molecular assessment of treatment effects;
 - ✓ more fundamental understanding of disease processes.
- The rat and mouse host a large number of human diseases
 - * Opportunity to study disease progression / therapeutic response
 - ✓ under controlled conditions
 - ✓ non-invasively
 - ✓ in same animal
 - ✓ repetitively

Mice advantages: small size, rapid gestation period large litter size, low maintenance costs. Moreover, the mouse genome has been extensively characterized. Gene-targeted "knock-out" and transgenic overexpression experiments are performed using mice, rather than rats, but submm spatila resolutin needed!



Molecular Imaging Modalities

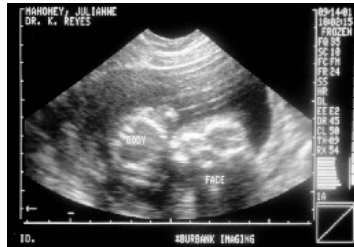


CT

Unique !!

A Tissue Density
20-50 μm

Ultrasound



A **F**
Structure
0.1 mm
Doppler

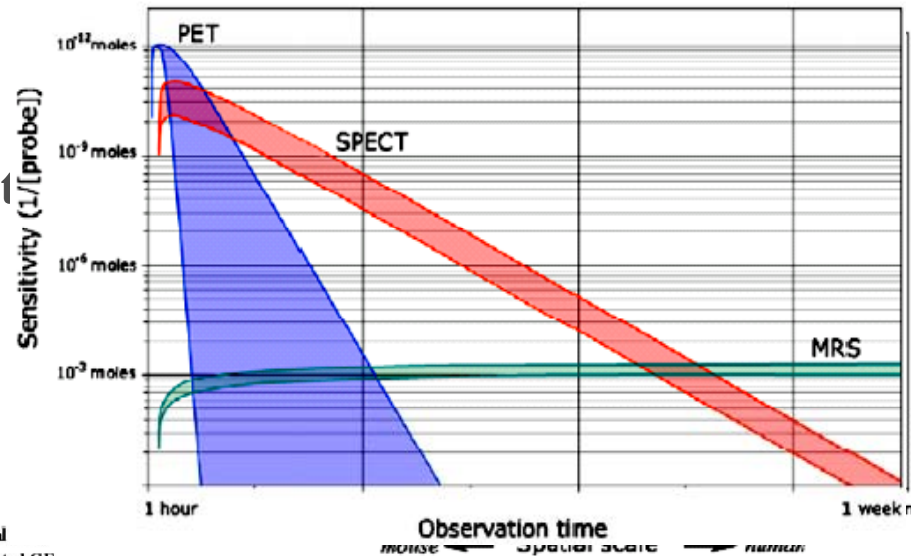
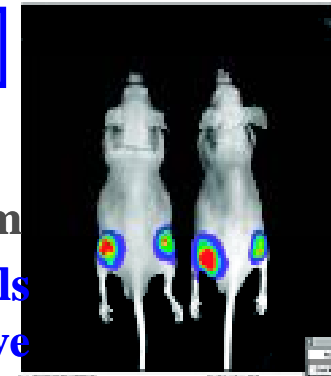
Optical

(Bioluminescence, fluorescence)

A **M**

Topography

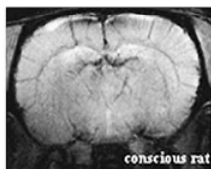
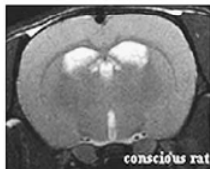
μm to mm
 $\sim 10^3$ cells
 \neq quantitative



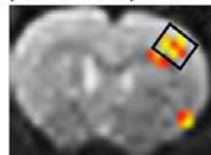
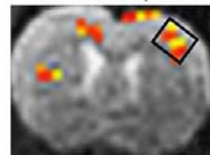
MRI

4.7T, Dual Coil, Coil,
T1 Weighted SE

4.7T, Dual
T2 Weighted SE



Activational Maps of Primary Somatosensory Cortex



A **F** **M**

H Concentration
0.1 mm

BOLD, DCE
 β -galactocidase

0.1 $\mu\text{mole H} / \mu\text{mole } ^{31}\text{P}$

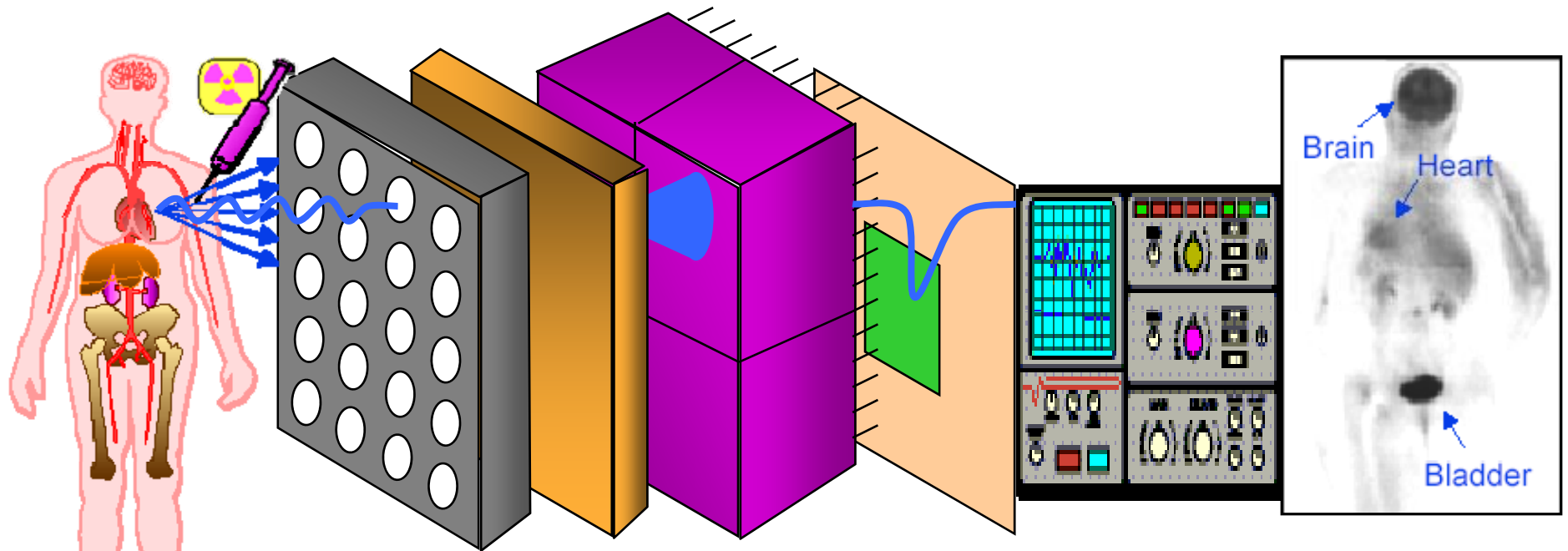
PET/SPECT

F **M**

Radiotracer
 $\sim 1\text{-}2$ mm
 $< 10^{-12}$ mole
 $=$ quantitative



Single Photon Detector Module



Patient injected with radioactive drug.

Drug localizes according to its metabolic properties.

Gamma rays, emitted by radioactive decay, that exit the patient are imaged.

1. Collimator

Only gammas that are perpendicular to imaging plane reach the detector

2. Scintillator

Converts gammas to visible light

3. Photodetector

Convert light to electrical signal

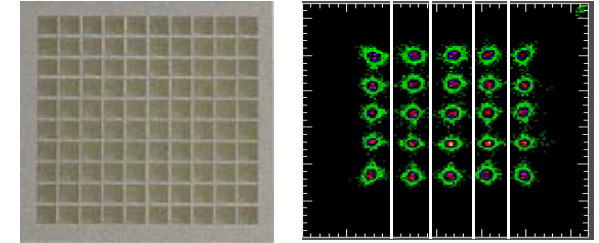
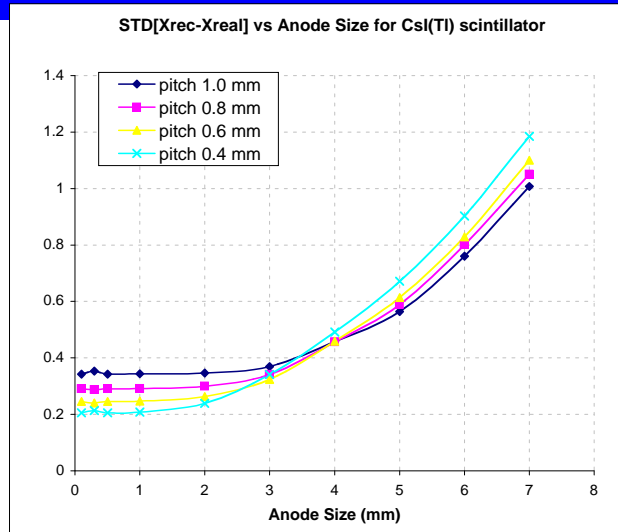
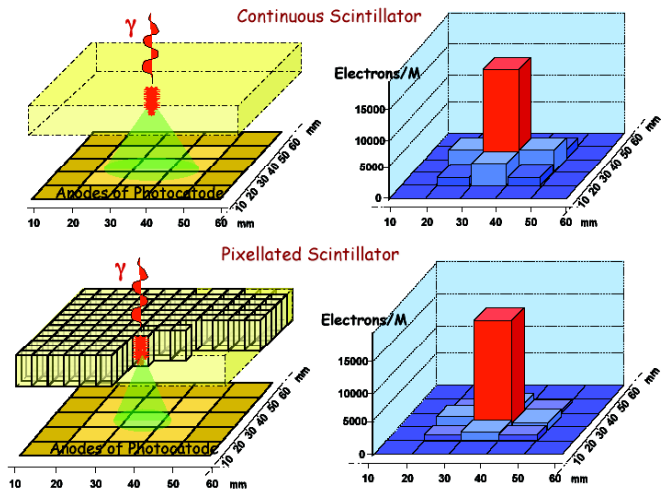
4. Readout Electronics

Amplify electrical signal and interface to computer

5. Computer decoding procedure

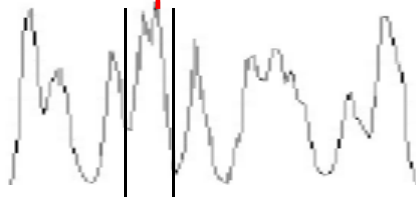
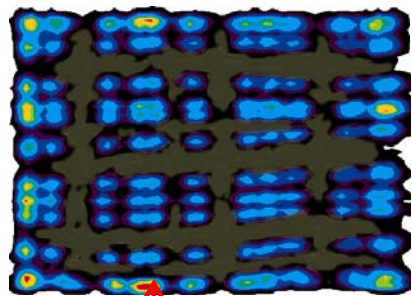
Elaborate signal and gives image output

Importance of pixel identification

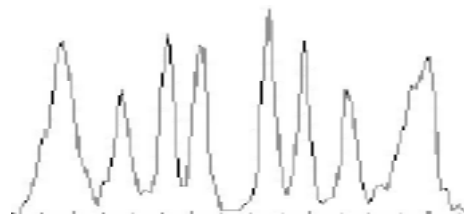
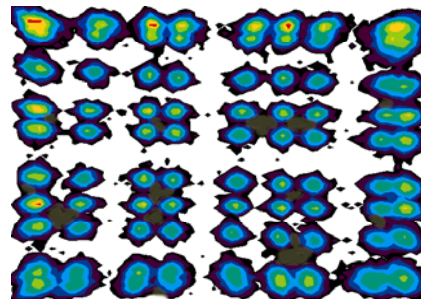


good pixel identification is fundamental for correct digitization affecting spatial resolution and contrast

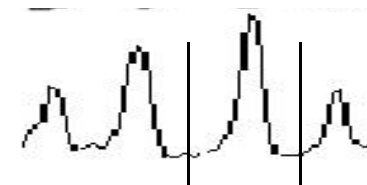
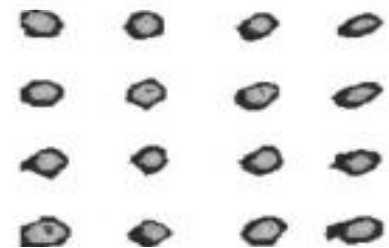
C8 strips



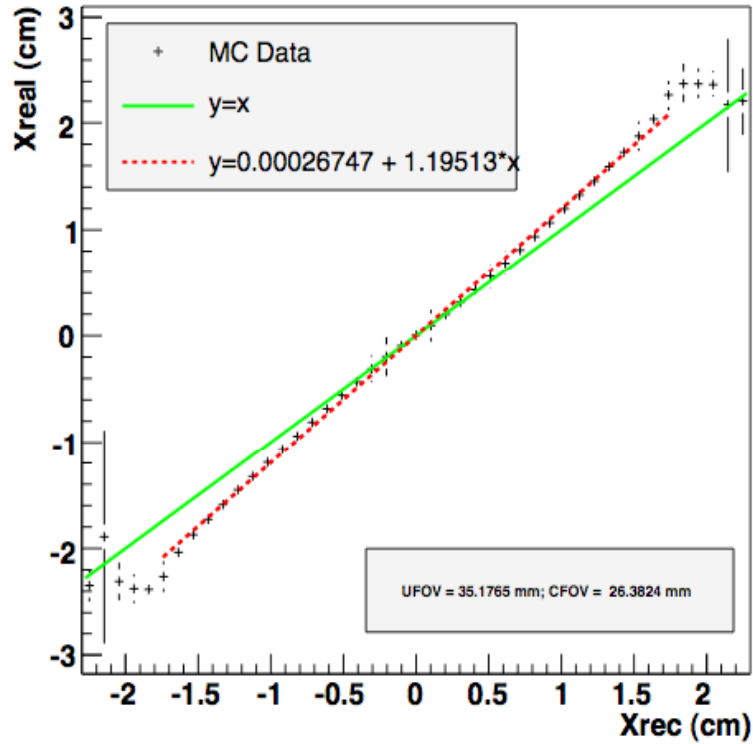
M16 (4 x 4) mm²



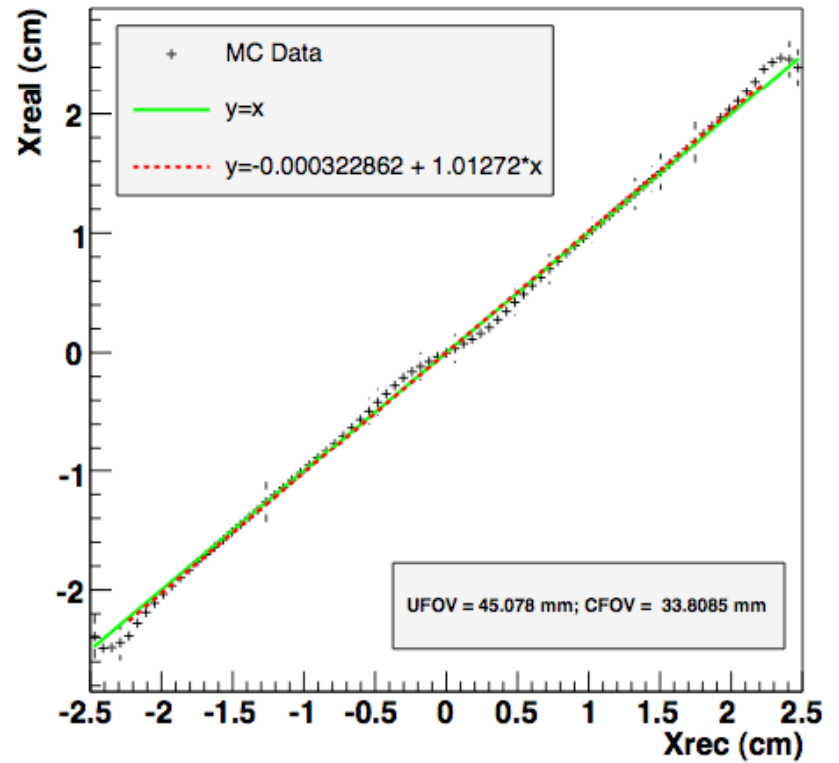
M64 (2 x 2) mm²



Labr3 Continuum different performances for different window treatment, diffusing (a), absorbing (b)



a



b

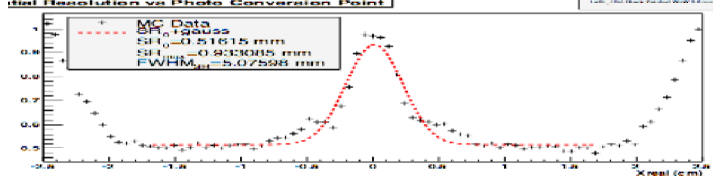
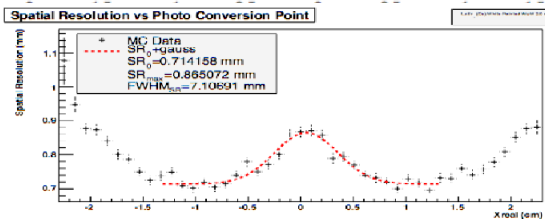
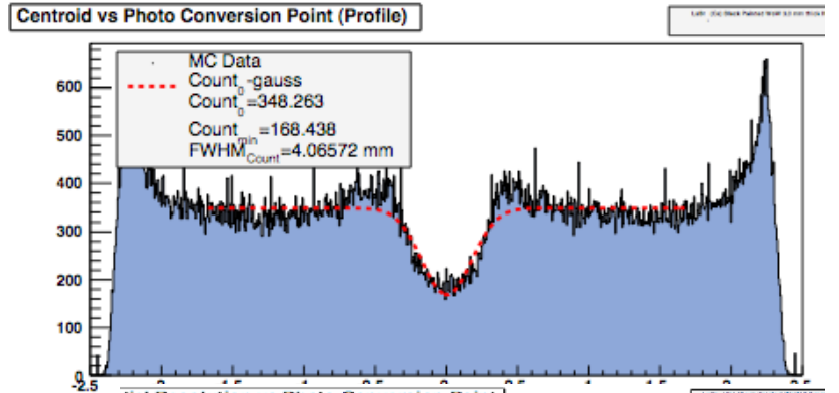
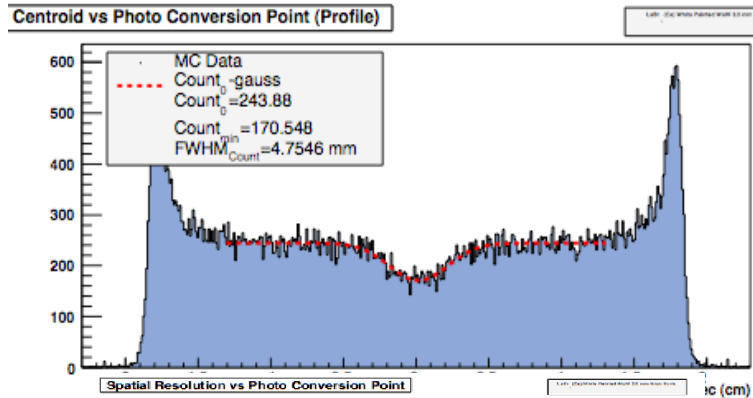
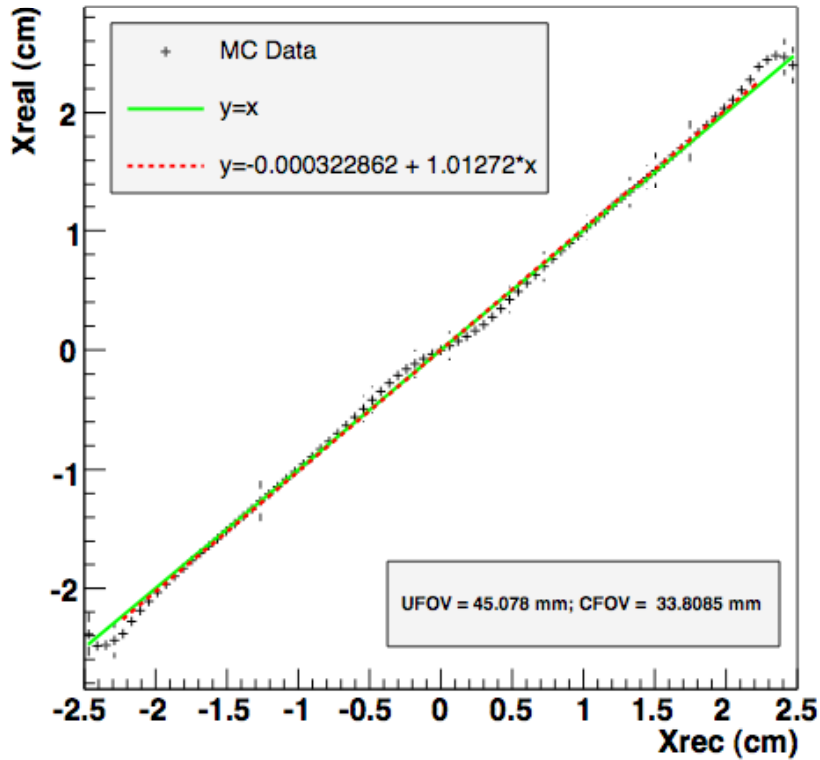
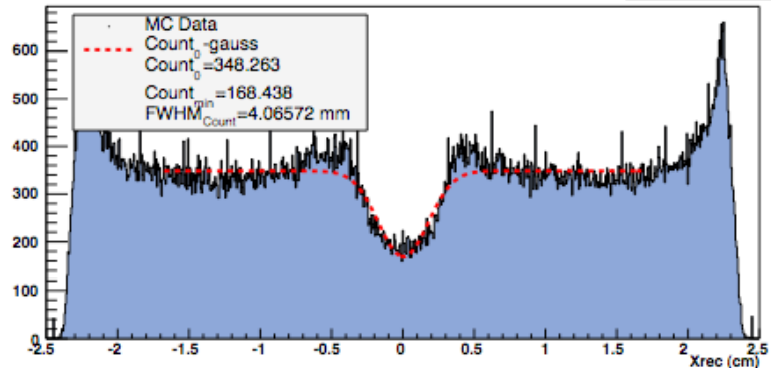


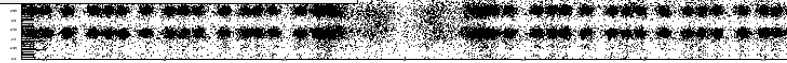
Photo Conversion Point vs Centroid



Centroid vs Photo Conversion Point (Profile)

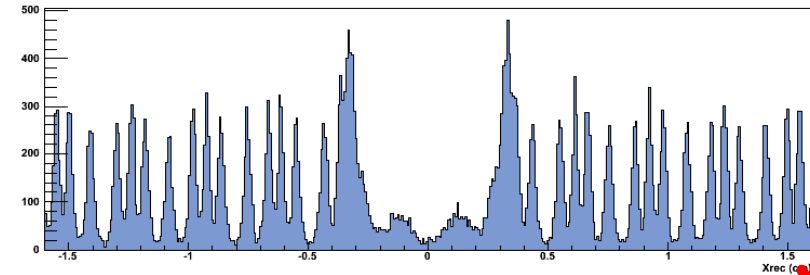


Scatter Plot of Reconstructed Positions

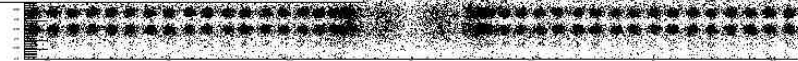


CsI(Tl) 0.8mm pitch, H9500

Centroid vs Photo Conversion Point (Profile)

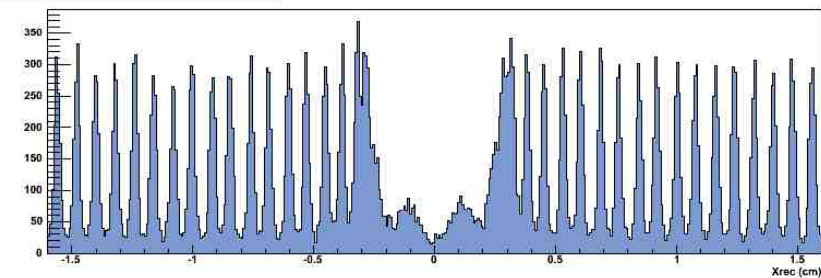


Scatter Plot of Reconstructed Positions



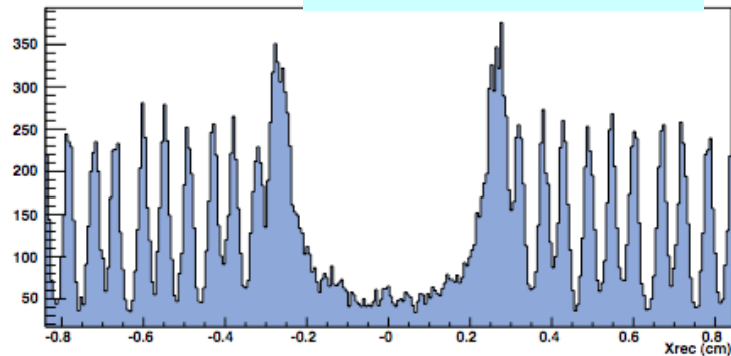
CsI(Tl) 0.8mm pitch Burle

Centroid vs Photo Conversion Point (Profile)



Centroid vs Photo Conversion Point (P

0.6 mm pitch Burle



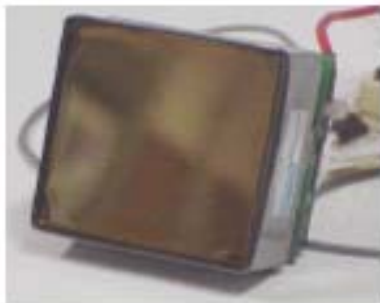
spatial resolution and linearity

- > number of p.e.
- > light spread
- > light sampling

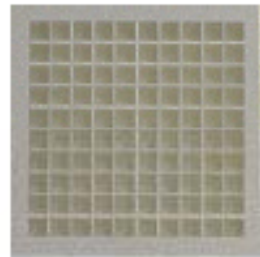
- scintillator thickness
- granularity



C8,
M16,
M64



H8500
H9500



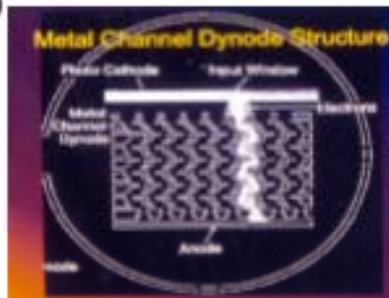
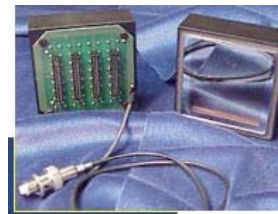
NaI(Tl): 1.2 pitch, 1.5 pitch
6 mm thick

CsI(Tl) 0.4 - 1.0 mm pitch

- R5900 C8 strips, 4 mm
- R5900 M16 4x4 mm²
- R5900 M64 2x2 mm²
- H8500 6x6 mm²
- H9500 3x3 mm²

MCP (Burle)
1.5x1.5 mm²

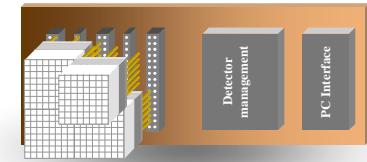
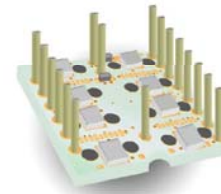
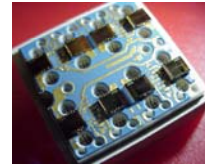
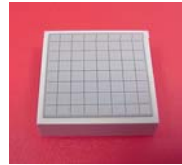
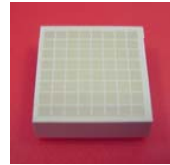
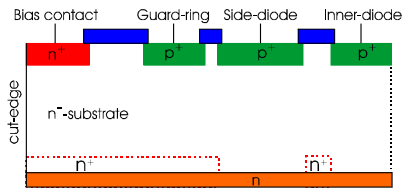
LaBr₃



Hamamatsu PSPMT's

readout of channels
individually is important
but
number of channels high

Silicon Drift Detectors



APD

APD array

Scintillator matrix (BGO/LSO)

Implemented on MADPET II

- + High spatial resolution
- + No Pile-up
- + No scattering in the crystals
- Expensive
- Many channels
- Difficult tuning

SiPM

SiPM are p-n diodes operating in **Geiger mode**, which means that the bias voltage is above the diode breakdown voltage.

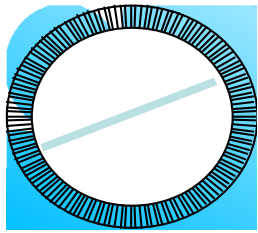
In this way output is independent from input:
 \Rightarrow the surface is divided into **m cells** ($\sim 1000/\text{m}^2$)

Signal $\propto N_{\text{cell}}$ of hit cells

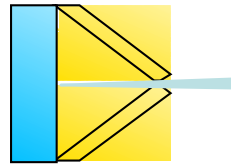
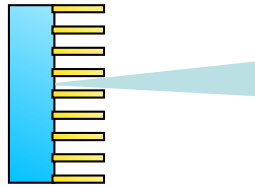
- + High gain
- + Low noise
- + Good proportionality if $N_{\text{photon}} < N_{\text{cell}}$

An array of SiPMs can be used for "individual" readout, instead of PSMP

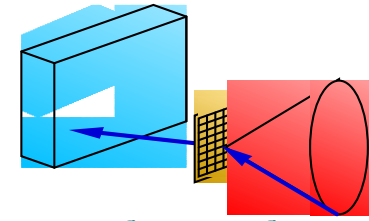
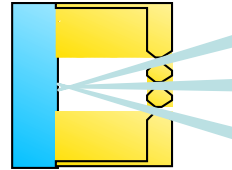
Si Pin diode: high QE, simple, economics, but no gain ! noise etc



pet

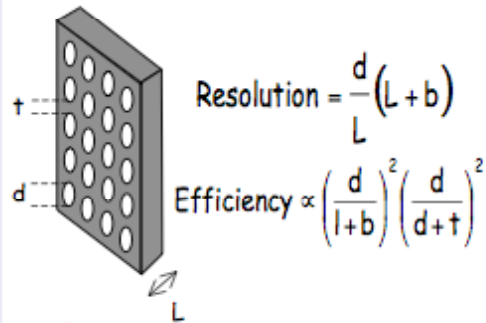
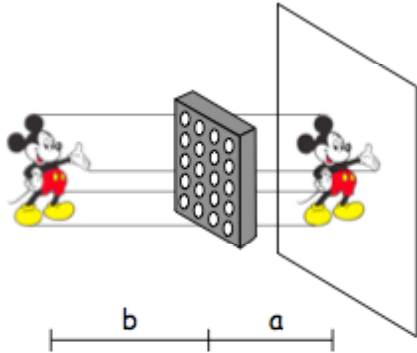


collimation



Compton Camera

Parallel Holes

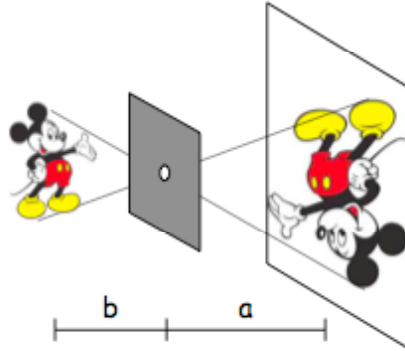


$$\text{Resolution} = \frac{d}{L} (L + b)$$

$$\text{Efficiency} \propto \left(\frac{d}{L+b}\right)^2 \left(\frac{d}{d+t}\right)^2$$

Resolution & Efficiency inversely related

Pinhole

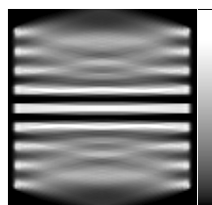


$$\text{Resolution} = d \left(1 + \frac{1}{M}\right)$$

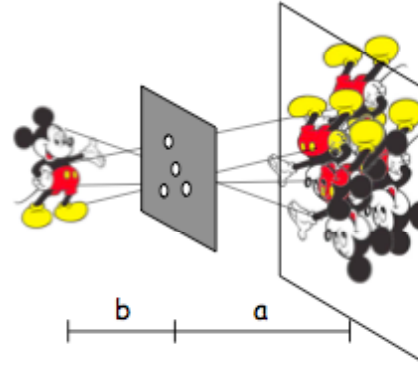
$$M = \frac{b}{a}$$

$$\text{Efficienzia} \propto \left(\frac{d}{4b}\right)^2$$

- 👍 Better Resolution
- 👎 Little Field of View
- 👎 Low Efficiency



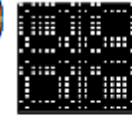
Coded Aperture



$$\text{Resolution} = d \left(1 + \frac{1}{M}\right)$$

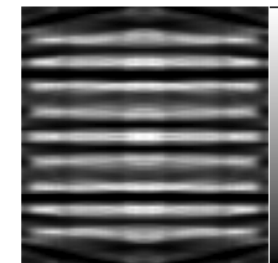
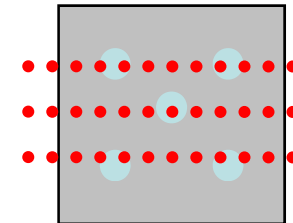
$$M = \frac{b}{a}$$

$$\text{Efficienzia} \propto N \left(\frac{d}{4b}\right)^2$$

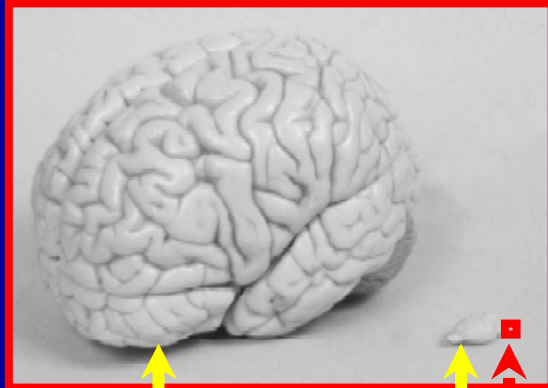


- 👍 Better Resolution
- 👍 High Efficiency
- 👎 Complicated Reconstruction

Multipinhole



Performances not good enough for imaging biological process in vivo in small animals (mice)



Human

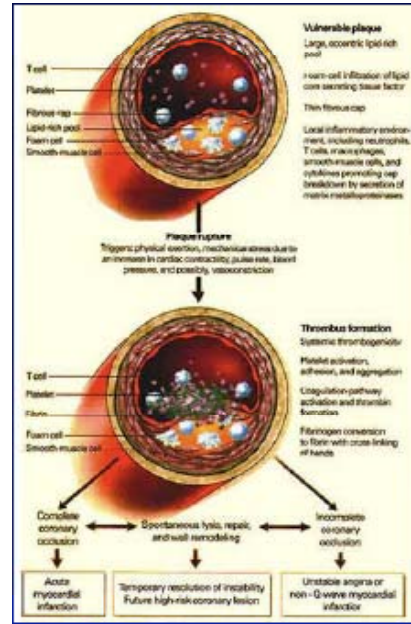
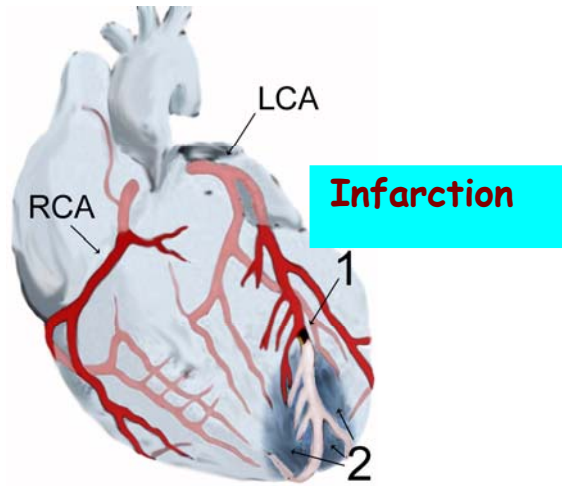
Rat

	Man	Rat	Mouse
Body weight	~70 kg	~200 g	~20 g
Brain (cortex apex-temporal lobe)	~105 mm	~10 mm	~6 mm
Heart	~300 g	~1 g	~0.1 g
Aortic cannula (□)	~ 30 mm	1.5 - 2.2 mm	0.9-1.3 mm (0.5 mm)
Required spatial resolution:	6 mm FWHM (200 mm ³)	2 mm FWHM (8 mm ³)	1 mm FWHM (1 mm ³)

- Small size detectors (high pixellization)
- Individual detectors or "perfect" coding

➔ **Submillimeter spatial resolution, high sensitivity needed**

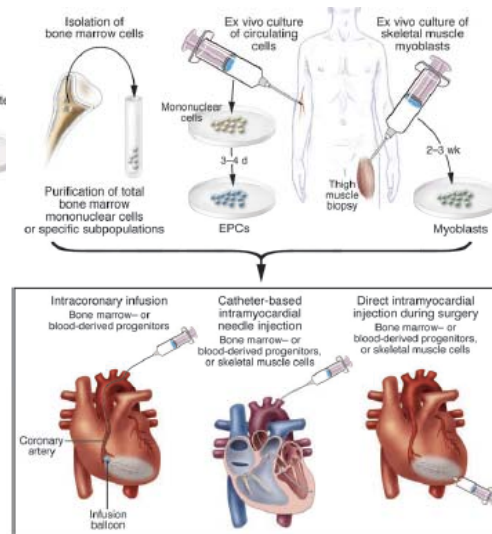
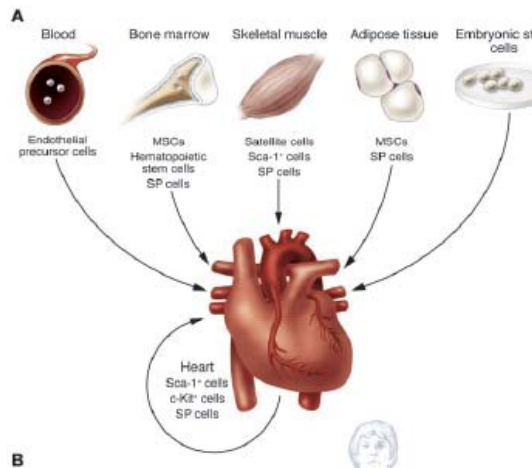
Cardiovascular diseases



Diagnosis

Detection of cause of occlusion

➔ *Imaging in vivo*: detection of vulnerable plaques



Therapy

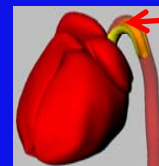
Stem cell therapy for cardiac repair

➔ *Imaging in vivo*: monitoring stem cells diffusion, differentiation, grafting, looking at the effects

APPROACH

- Transgenic mouse model
 - APOE^{-/-} mice
 - Spontaneous growth of atherosclerotic plaques accelerated by fatty diet
- Imaging agent
 - ^{99m}Tc-HYNIC-Annexin-V (Binds to apoptotic cells)

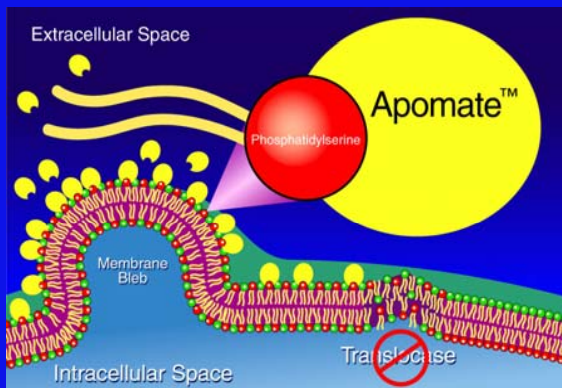
- ~ 2 mm diameter aorta
- ~ 0.5 X 1 X 4 mm³
- Total activity: ~ 1 microCi, (0.05% of average injected dose of ~2 mCi)



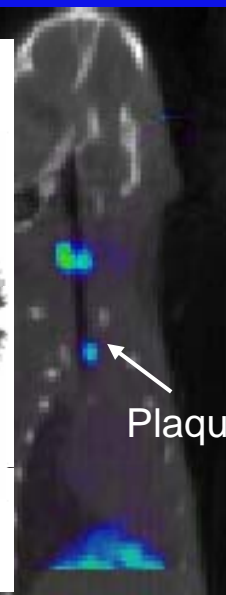
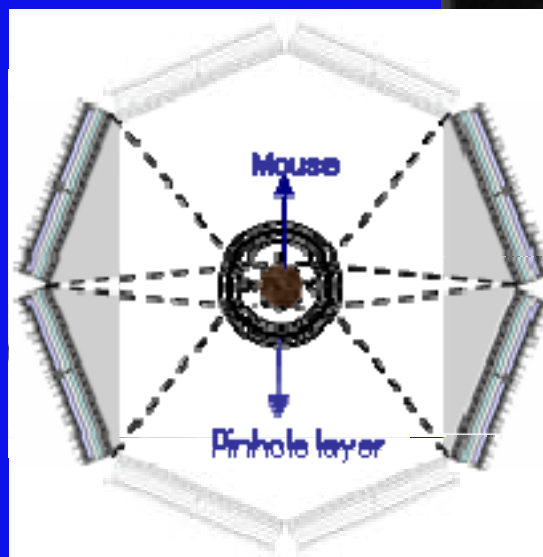
plaque

^{99m}Tc-Annexin-V SPECT images

Excised aorta from 37 weeks mouse



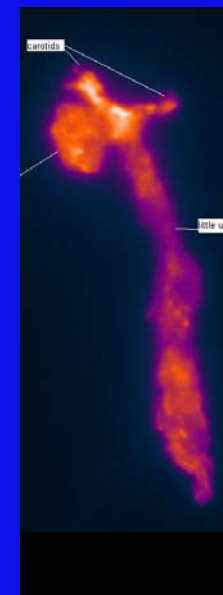
Apomate™: Trade name for Hynic Annexin V, North American Scientific, Inc.



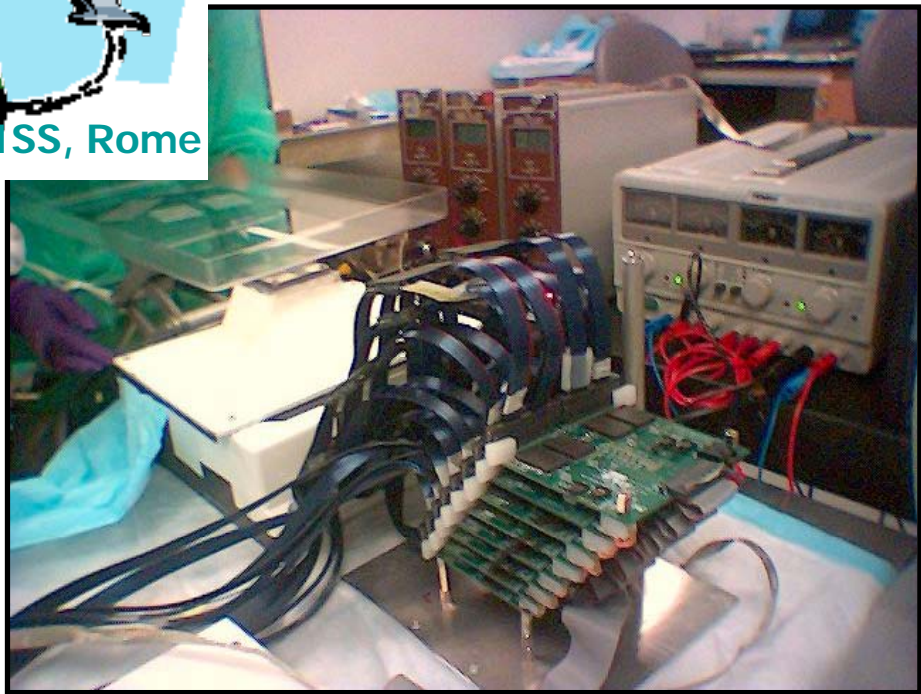
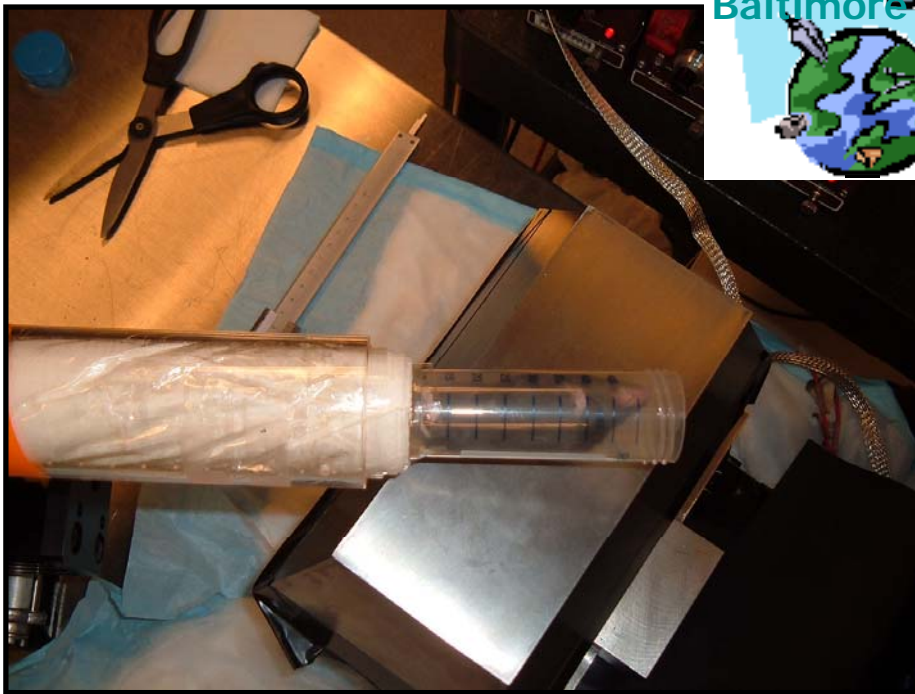
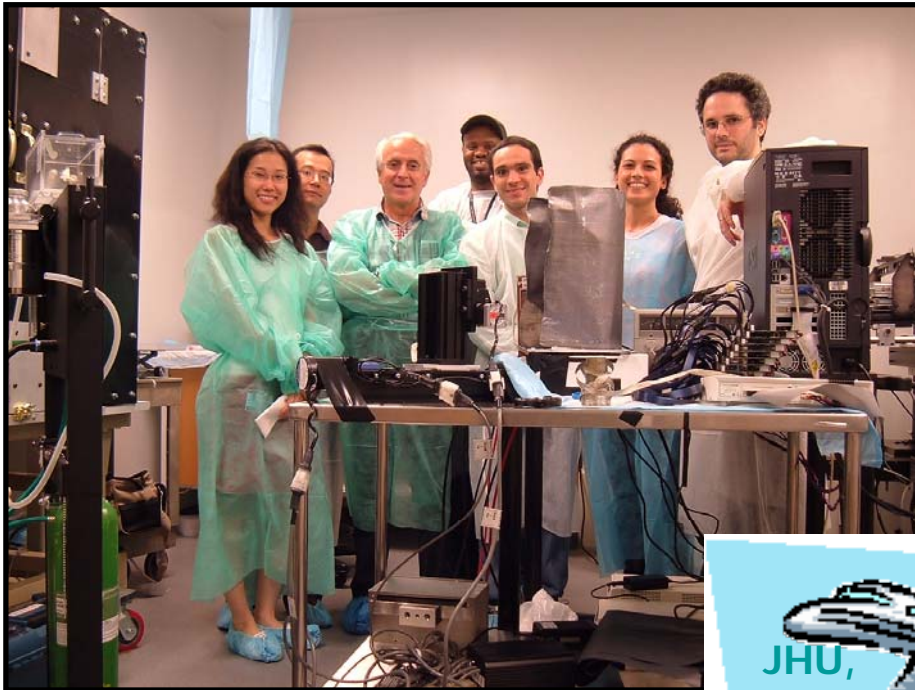
20 weeks

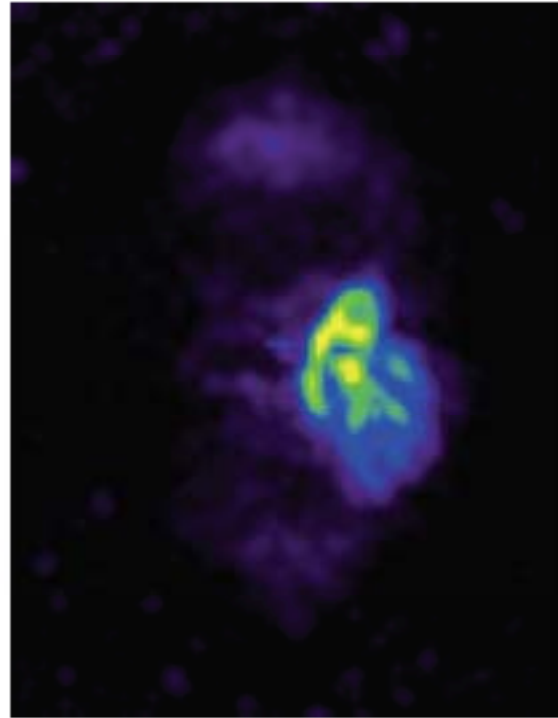


Photo

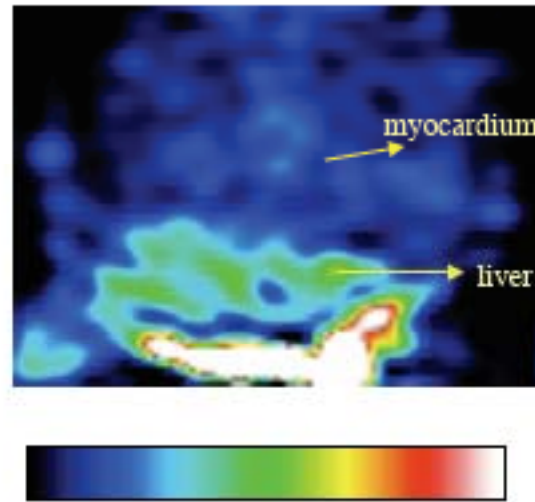


autoradiography

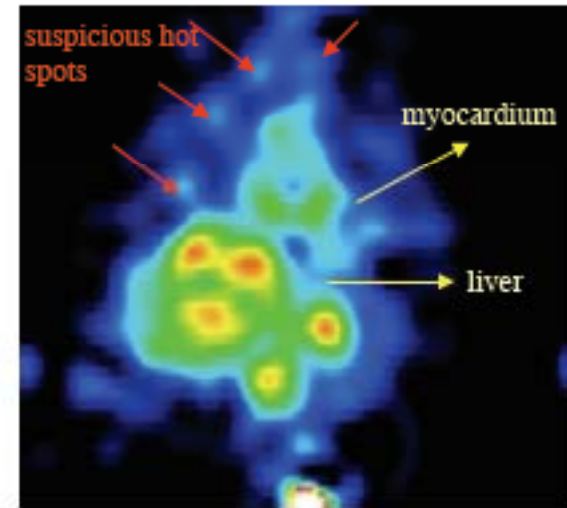




a. Topo di 6 settimane



b. Topo di 25
settimane
control



c. Topo di 25 settimane

Fig. 25. Immagini di topi geneticamente modificati (APOE $-/-$) cui e' stata iniettata Annexin V marcata con Tc-99. a. Uptake solo dal rene; b. non c'e' uptake da placche, si vede chiaramente il miocardio c. Si vede chiaramente l'uptake da placche aterosclerotiche

A

Blood Bone marrow Skeletal muscle Adipose tissue Embryonic stem cells



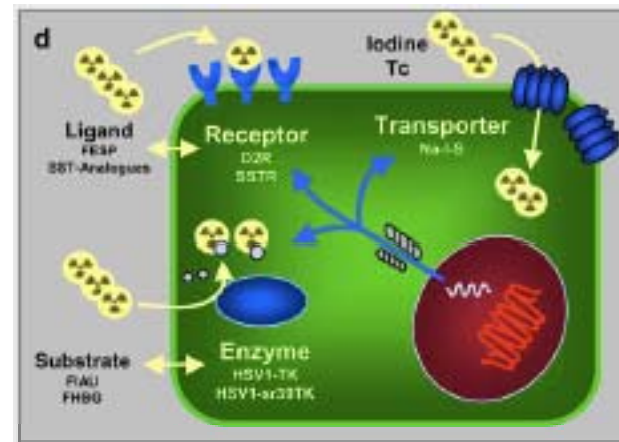
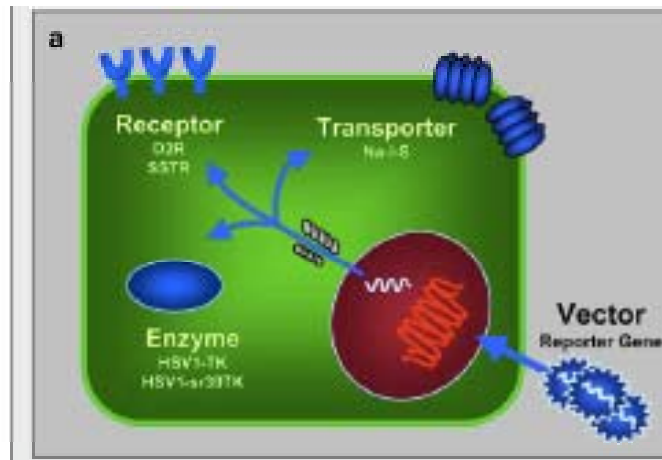
Develop and validate imaging tools for novel cell therapies (e.g. immune cells or stem cells) allowing tracking of cells and assessment of cell fate (e.g. viability, differentiation, migration and therapeutic effects, that could be tested in animal models with a view towards translational medicine. The development tools should provide specific and quantifiable information with respect, for example, to cell homing, functional read-outs, tracking of differentiation or immune system response .FP7

These reports underscore the need for a greater understanding of the mechanisms underlying stem cell biology and cellular reparative therapy, and their potential uses in the post-infarction state.

This proposal aims to elucidate the mechanism of action behind stem cell activity in cardiac regeneration, an area of tremendous contemporary pre-clinical and clinical activity. This ambitious proposal targets one of the most important questions arising in this field using a multiple way approach. The complex and innovative strategy to elucidate the mechanisms of stem cell mediated cardiac repair is highly valuable and could be beneficial for further development of pragmatic therapeutic strategies in this clinically relevant area. Such approach is complemented by the intention to develop multimodal molecular imaging technologies, primarily integrating SPECT with MRI. This technically difficult and challenging task would, if successfully accomplished, open new possibilities for the whole area of interest. Some aspects of this and other working tasks would,

- Optical 10^{15} to 10^{17} mol/l
- PET, SPECT 10^{11} to 10^{12} mol/l
- MRI 10^5 mol/l

direct labeling: labels may be diluted upon cell division, making these cells invisible; and labels may efflux from cells or may be degraded over time.



alternative approach: stable transfection of cells with a **reporter gene**, such as herpes simplex virus type-1 thymidine kinase (HSV1-tk), whose expression can be visualized using a radioactive PET or SPECT reporter probe
(phosphorylates --> TK --> triphosphate --> cells)

PET and SPECT imaging can be used to assess cell trafficking, function, and efficacy, using methods which are easily **translatable to humans**. Reporter gene approaches are particularly valuable, as they provide information **not only on cell trafficking**, but also on **cellular function and survival**

Dual labeling

- **Optical imaging** techniques provide high spatial resolution and permit tracking of stem cells but are limited to preclinical use
- **Magnetic resonance** imaging methods permit good spatial resolution but limited detectability
- **Nuclear techniques**, including reporter genes and direct cellular radiolabeling, afford very good detectability but more limited spatial resolution

A multimodality approach using combined PET or SPECT and MRI agents may ultimately prove most useful in clinical settings.

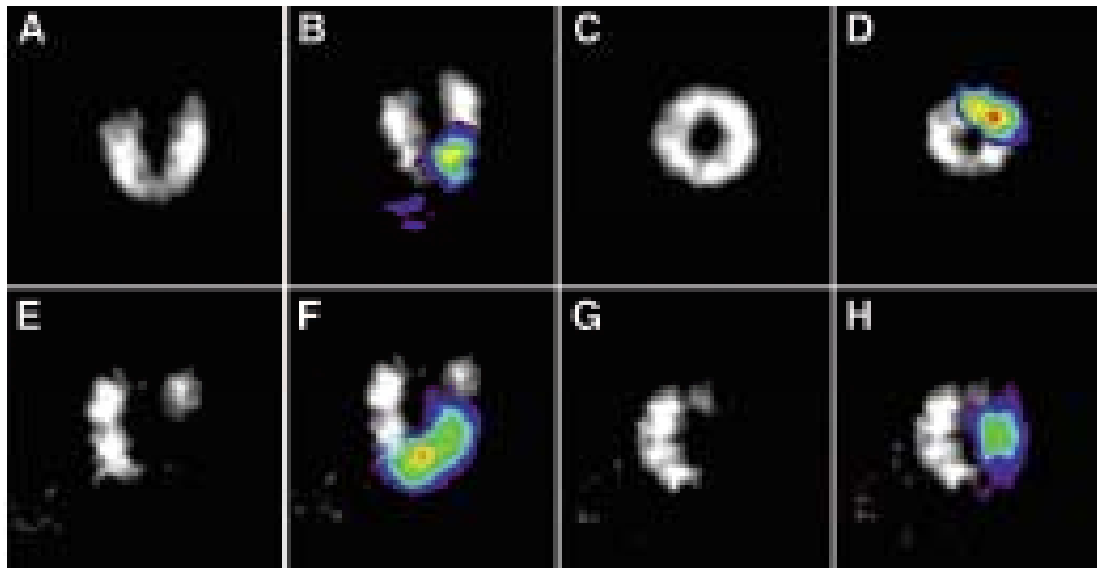
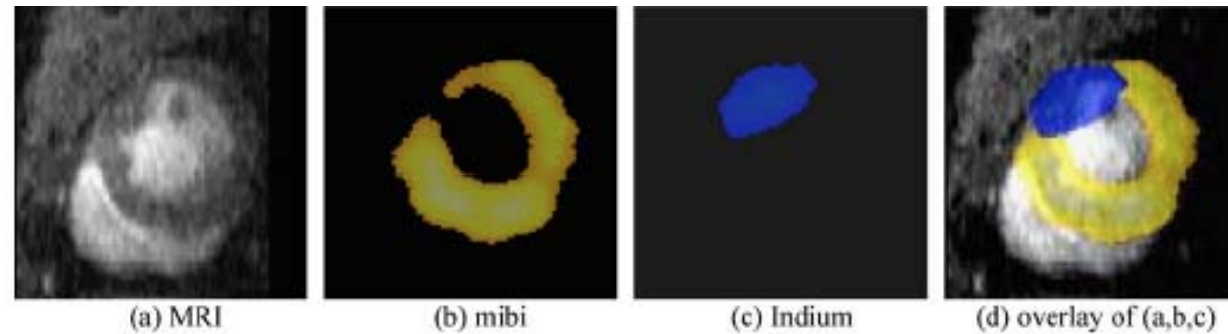


FIGURE 1. Cardiac long- and short-axis SPECT images of normal (A and C) and infarcted (E and G) heart using perfusion tracer ^{99m}Tc -sestamibi. ^{111}In signal (color) was overlaid on gray-scale ^{99m}Tc -sestamibi images for normal (B and D) and infarcted (F and H) heart.

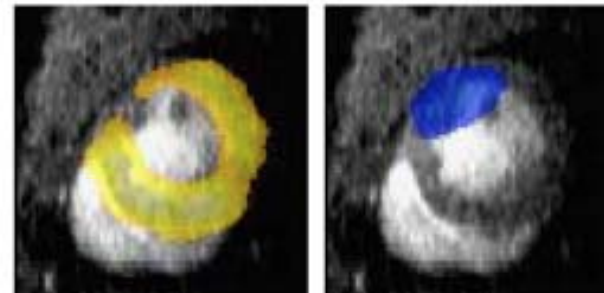
P. Acton and al.

and Multimodality

(Zhou, Acton)

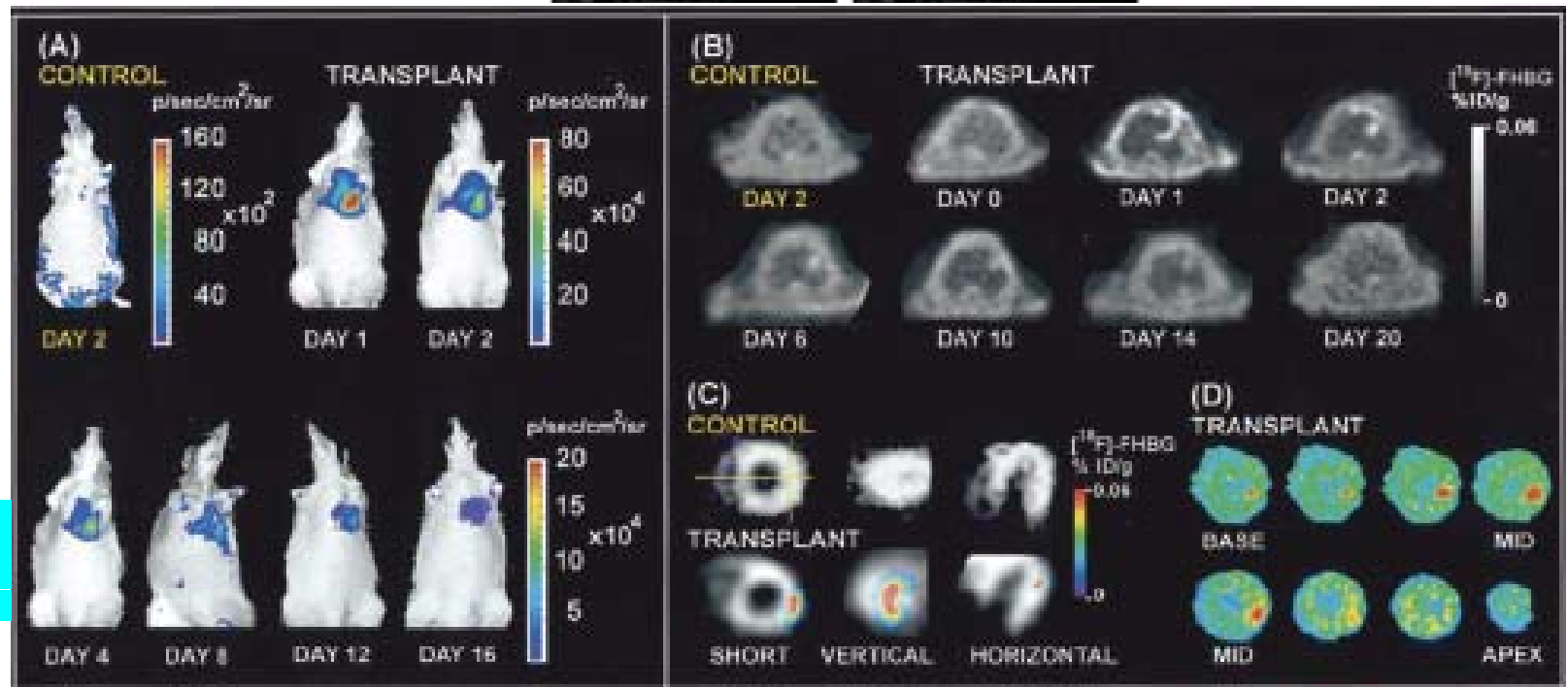


SPECT/MRI



OPTICAL/PET

(Gambir)

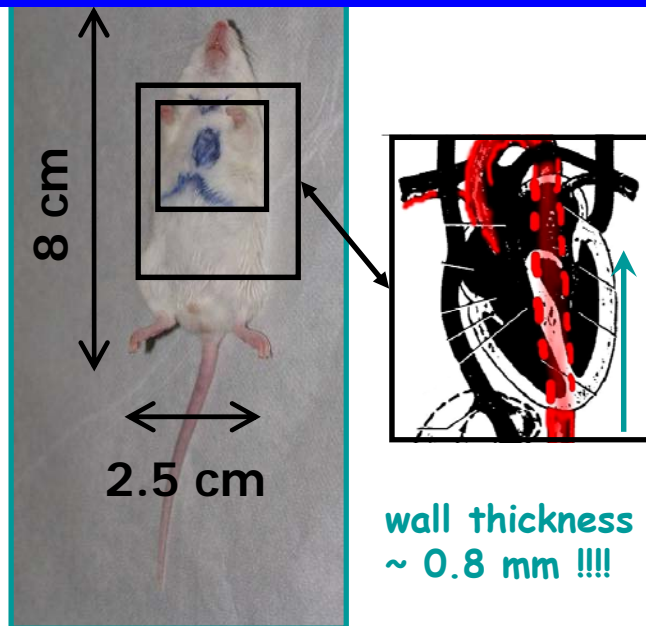


↪ **Detector** ~ 100x100 mm²
↪ **Intrinsic resolution:** 1.2 - 1.5 mm
↪ **pinhole** (0.5 mm)

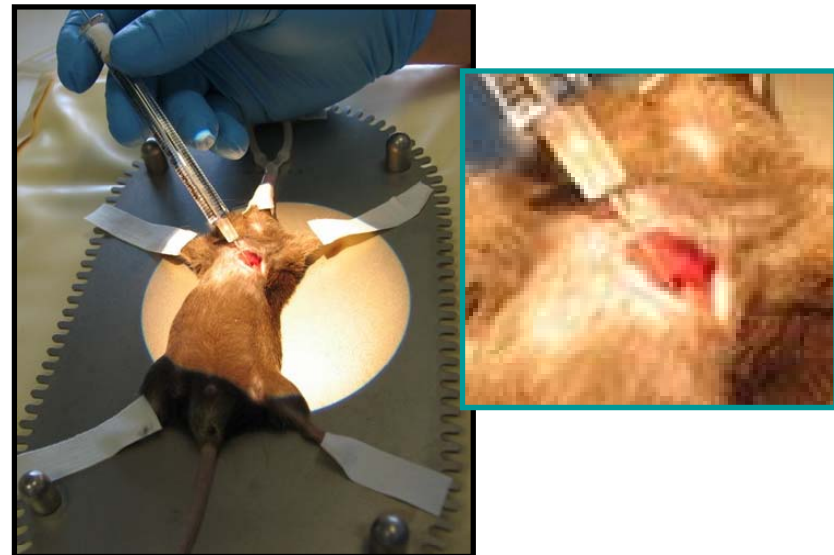
high resolution : ~ 0.8 mm

↪ **M= 3** ==> **FoV** ~ 33 x 33 mm²

↪ **Perfusion Imaging**



↪ **Tracking and homing of stem**



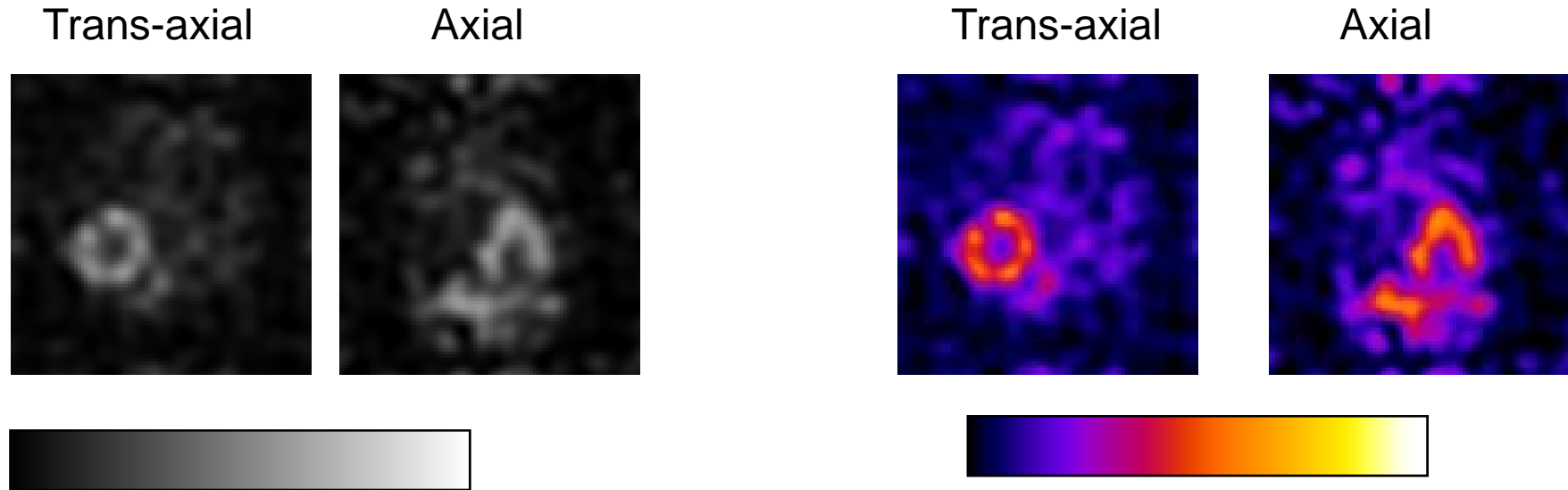
mouse: C57 BL/6, male

age: ~ 12 weeks

weight: ~ 31.5 g

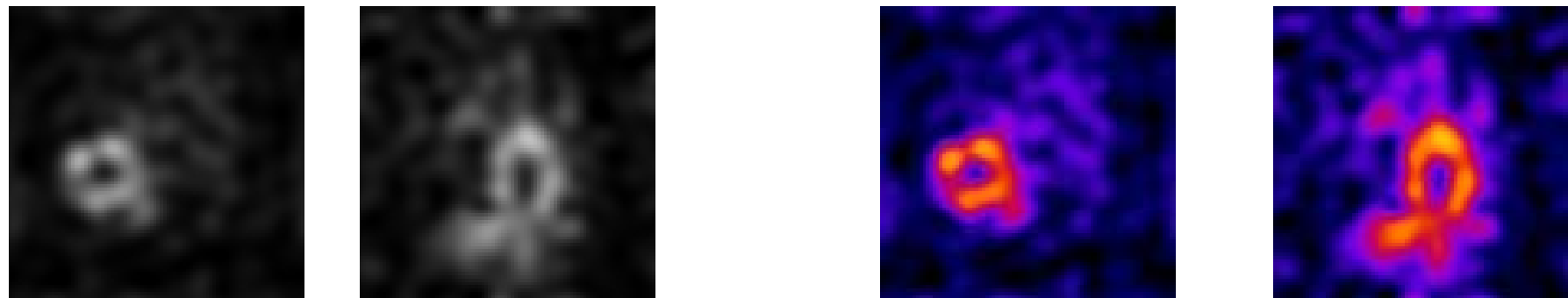
stem cells: ~ 6×10^4 murine (SCA+/KIT+ Tc^{99m}-HMPAO (28 microCi)

Reconstruction Images of Mouse Perfusion Scan (I)



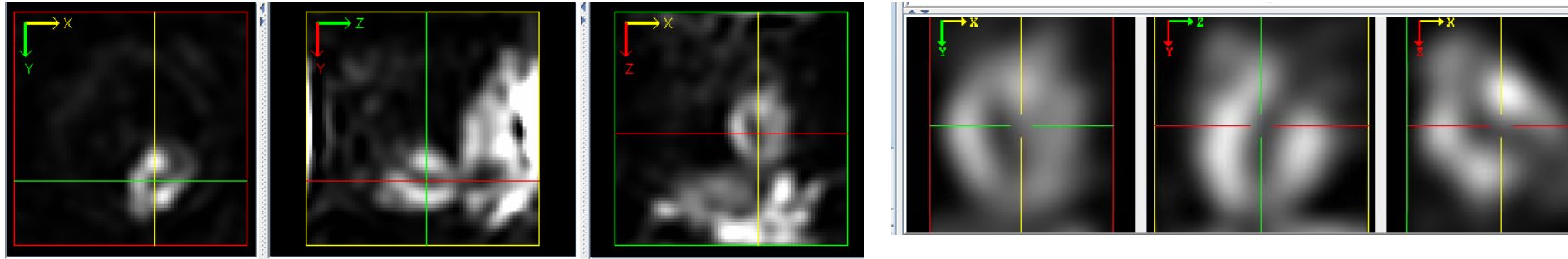
OS-EM, 6 subsets, 2 iterations, post-smoothed by
Butterworth filter (cutoff=0.12, order=8), voxel size =
0.25 mm, image dimension 90x90.

Reconstruction Images of Mouse Perfusion Scan (II)

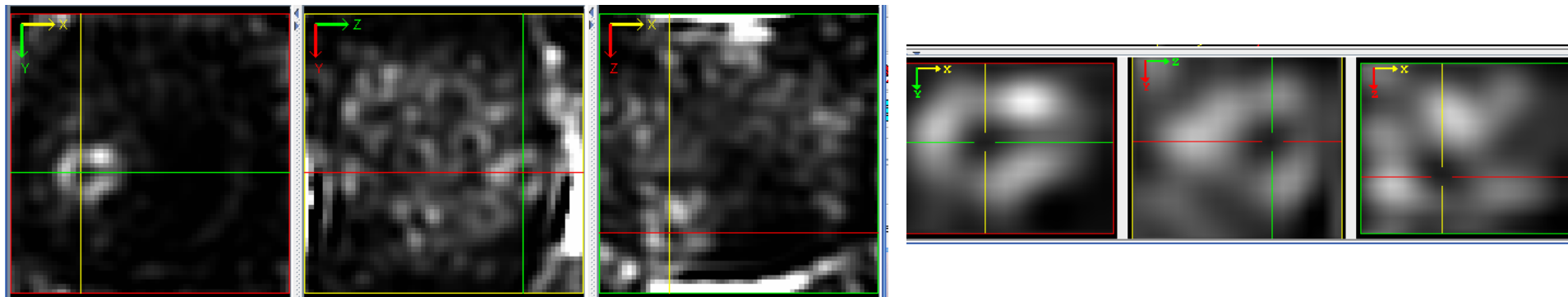


Transverse (X-Y)	Sagittal (Y-Z)	Coronal (X-Z)
------------------	----------------	---------------

Tail vein injection



Peritoneum injection



It is extremely difficult if not impossible to use the tail vein for radiotracer many times. An alternative route of delivery is needed, but, how much will arrive to heart? Let's look at the peritoneum.

It works, but there is a price to pay, the uptake is decreased (a factor of ~ 2).

We have to maximize the efficiency

→ More detectors

→ Multipinhole

Conclusions

Importance of molecular imaging in the biomedical research panorama: crucial role of radionuclides techniques

Multidisciplinary approach mandatory

Multimodality ("new" photosensors (SiPm?))

- atherosclerosis:

- looking for smaller plaques "earlier" detection (other mechanisms, other radiotracers)

- stem cells:

- selecting "right" cells
- monitoring diffusion, differentiation, grafting etc
- looking at the effects

==> multimodality (optical, SPECT, MRI,)

Outlook

-the challenge: 120 pixel/100 mm, 8 modules 150 X 100 mm²

----> FOV 50 x 33 (M=3))

Richiesta per il 2009



50x50 mm² CsI(Na)
0.8 mm pitch
M = 2, FoV = 25x25 mm²

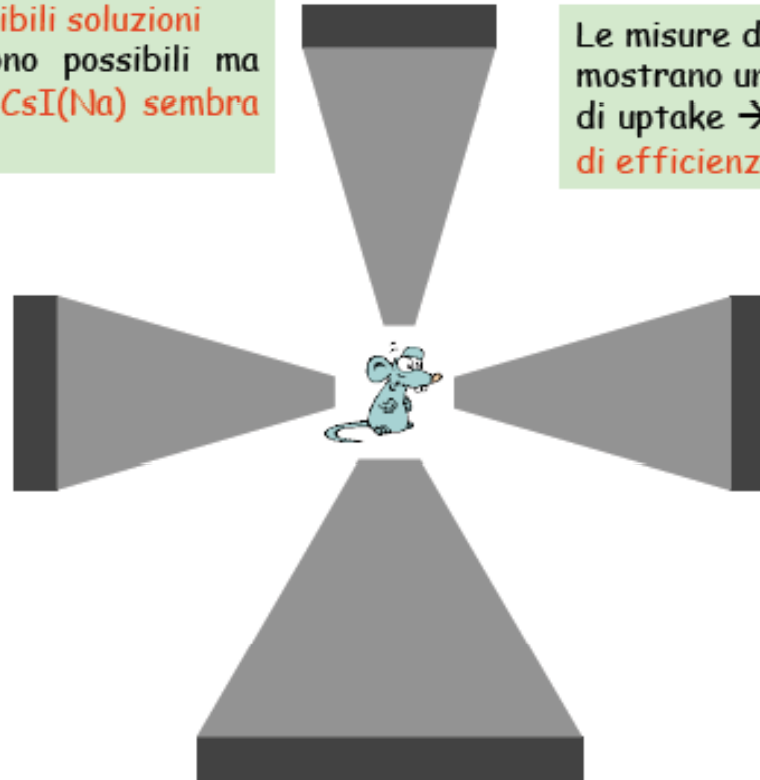
Confronto tra 3 possibili soluzioni
CsI(Tl) e LaBr₃ sono possibili ma
diversi problemi. Il CsI(Na) sembra
la soluzione migliore

Le misure dopo iniezione in peritoneo
mostrano un significativa diminuzione
di uptake → necessita' di valutazione
di efficienza con misure su topi

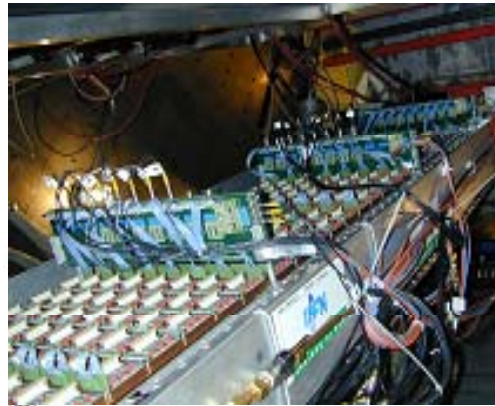
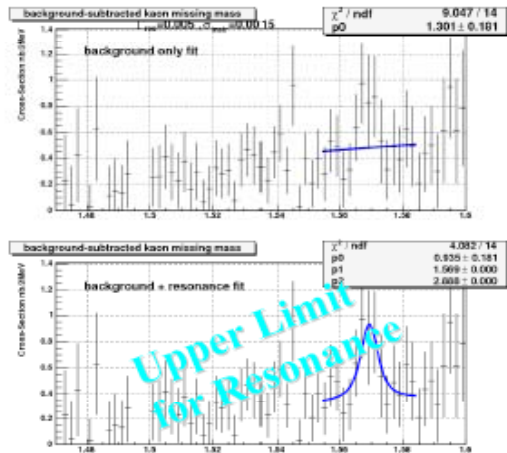
50x50 mm² CsI(Tl)
0.8 mm pitch
M = 2,
FoV = 25x25 mm²

50x50 mm² LaBr₃(Ce)
4 mm thick,
3 mm thick window
M = 2,
FoV = 25x25 mm²

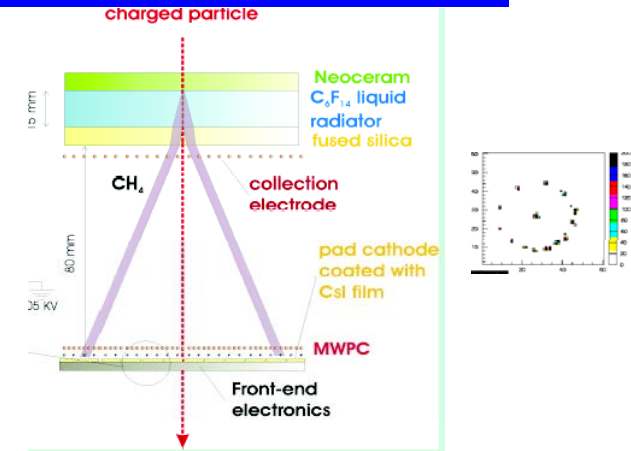
100x100 mm² NaI(Tl)
1.2 mm pitch
M = 3, FoV = 33x33 mm²



Θ^{++} Search



Freon/CsI RICH detector (like ALICE)



Spectroscopy analysis of $^{12}\text{B}_\Lambda$: Aerogel vs. RICH K-selection

$$\frac{d\sigma}{d\Omega}(\gamma^* p \rightarrow \Theta^{++} K^-) |_{\theta=2^\circ} < 3nb$$

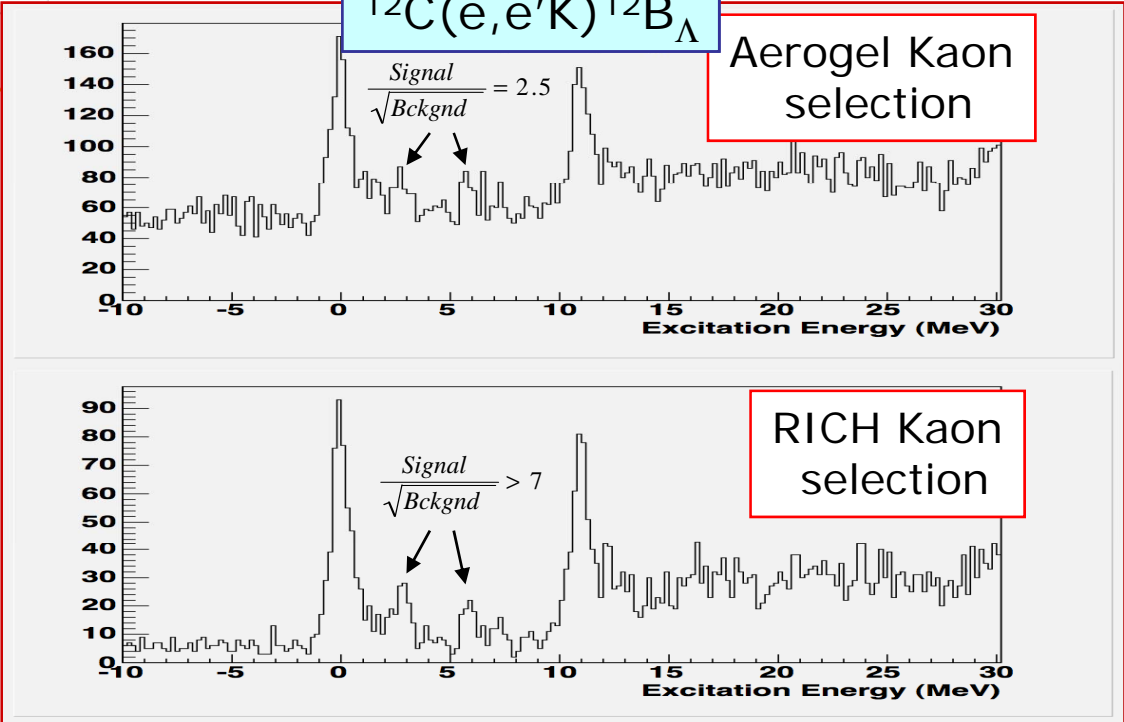
Hermes aerogel RICH

HERMES
3870 PMTs, Philips XP1911/UV, Ø 3/4" + light funnels

Online Event Display
TOP RICH

$\langle N_{p.e.}(\text{aerogel}) \rangle = 8$
 $\langle N_{p.e.}(\text{C}_4\text{F}_{10}) \rangle = 12$

E. Nagy



Important parameters for detectability/visibility

$$SNR = \frac{S - BKG}{\sqrt{S}}$$

efficiency collimation
time (and modality)
uptake (radiopharmacy)

$$X = \frac{\sum_{i=1}^{N_{\text{channel}}} c_i X_i}{\sum_{i=1}^{N_{\text{channel}}} c_i}$$

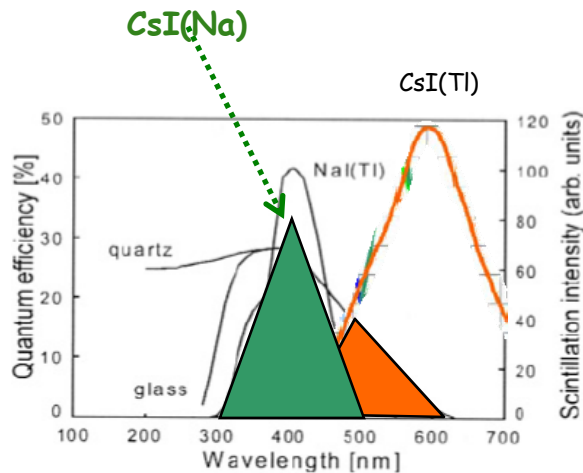
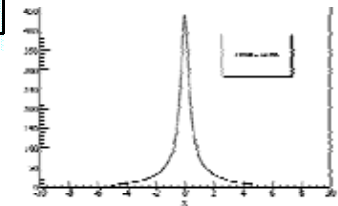
spatial resolution

$$IC = \frac{Max - BKG}{Max}$$

detector intrinsic properties
modality (compression)

scintillator
pixel dim/n. of pixels
electronics, DAQ

Uniformity of p.h. response
(affects the overall en res. and the energy window section)



Scintillators

		NaI(Tl)	CsI(Tl)	YAP	LaBr ₃ (Ce)
Density	g/cm ³	3.67	4.51	5.55	5.29
Effective Z	Bialkali PMT	51	54	32	47
Relative Yield	%	100	45	35-40	130
Peak Wavelength	nm	410	550	360	360
$\Delta E/E$ @ 140 keV	%	9	15	20	6
μ @ 140 keV	cm ⁻¹	2.7	3.9	1.7	3.0
τ @ 140 keV	cm ⁻¹	2.1	3.2	0.9	2.2
Thickness (90% eff)	mm	8.7	6.0	13	

τ/μ fotofraction

$$\sigma_X \propto \frac{\sigma_{X_i}}{\sqrt{N_{p.e}}} \Rightarrow R \equiv FWHM_X \propto \frac{FWHM_{X_i}}{\sqrt{N_{p.e}}}$$

CsI and LaBr₃ selected as possible optimal candidates:

- Submillimeter CsI Pixels available
- LaBr₃ is very promising (available in tiles of $\sim 5 \times 5$ cm²)